Effective Point of Reflection Changes in ALPS-IIc Mirror Coatings

Ethan J. Taylor
Max-Planck-Institut für Gravitationsphysik (Albert-Einstein-Institut), Leibniz Universität Hannover
University of Florida and University of Wyoming

(Dated: 01 Aug 2018)

The ALPS experiment seeks to discover axions or “weakly interacting sub-eV particles” (WISPs) through an experiment in which photons are oscillated into axions and then oscillated back into photons, using large magnetic fields and high finesse Fabry-Perot cavities with identical optical modes. In order to maintain high transmitted power throughout the experiment, the length of the regeneration cavity must follow the production cavity length, and due to the use of 1064 nm and 532 nm light, the cavity lengths are different for each wavelength due to different depths of reflection. The Effective Point of Reflection experiment tests the proposed mirror coatings for ALPS-IIc and their ability maintain the 95% power transmission requirement for ALPS-IIc. In this paper the current progress of the Effective Point of Reflection experiment is presented and future steps are discussed.

I. INTRODUCTION

The Standard Model of particle physics, while far reaching and accurate in its descriptions of three of the four fundamental forces is still not fully cohesive, despite its ability to allow for experimental predictions. The shortcomings of the Standard Model, such as the inability to describe gravity or the supposed lack of dark matter in the universe are just two of the issues. Some of these shortcomings can be solved through the introduction of a new particle into the model, the axion.

Introducing the axion to the Standard Model provides a solution to the Strong CP problem of particle physics, and also provides a candidate for cold dark matter in the universe[1,2].Naturally, this makes axion searches a very worthwhile endeavor, and multiple experiments have been done in an attempt to discover it[3]. There are experiments exploring the NMR signal of axions (Cosmic Axion Spin Precession Experiment, CASPEr), experiments exploring the possible axions emitted from the Sun, and more. This paper focuses on the ALPS-IIc experiment for axions, a purely laboratory experiment meant to explore the lower bounds of the ALPs (Axion-like-particles) photon coupling strength, while having the ability to be a completely laboratory controlled experiment.

A. ALPS-II

ALPS-II is an LSW (Light-Shining-through-Wall) experiment that is a significant upgrade of the previous ALPS-I experiment, which while it did not detect ALPs, it reached new levels of sensitivity and excluded ALPs with a coupling strength above $g_{a\gamma\gamma} = 5 \times 10^{-8} GeV^{-1}$.

This experiment wishes to discover ALPs through the exploitation of ALPs to photon coupling, in which a photon is coupled to an ALP through the application of a perpendicular magnetic field (i.e. a photon disappears through oscillation into an ALP), the ALP traverses a “wall” through which photons cannot pass, and then the ALP reconverts into a photon to be detected on the other side of the wall. This setup can be easily realized in Fig. 1, where the photons are transmitted through a magnetic field of strength B_0 over a path length L, converted to ALPs, and then reconverted to photons on the opposite side to be detected. As discussed in [Graham

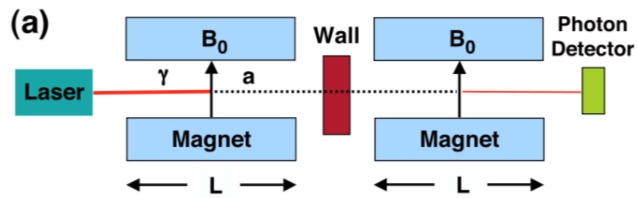

FIG. 1: Basic LSW Setup[4]

et al.[3], Sikivie, Tanner, and van Bibber[4], Ehret *et al.*[5]], the coupling strength is very weak, and can only be sufficiently increased by increasing the product of L and B_0. By introducing cavities into the path, which allow for coherently recycled light, as shown in Fig. 2, lower coupling strengths are able to be probed by utilizing the recycled power of the cavity. The steps to obtain the up-

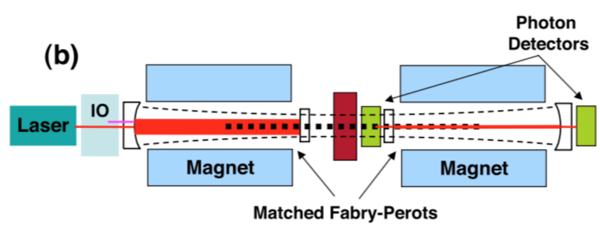

FIG. 2: Cavity LSW Setup[4]

per bounds of axion sensitivity are then obtained through the maximization of the magnetic field strength, the photon traversal length, the input power, the finesse of the cavities, and the efficiency of the individual components (mirrors, photon detectors, etc.).

Using the far field approximation described in Graham *et al.*[3] it is found that the probability of a two photon oscillation is not only dependent on the photon energy and the mass of the WISP, but also on the length of the experimental area and the finesse of the cavities, as shown in Eq. 1.

$$P_{\gamma\to\phi\to\gamma} = \frac{\omega}{\sqrt{\omega^2 - m_\phi^2}} \cdot |C_{wisp}|^4 \cdot \mathcal{F}_{\mathcal{PC}} \cdot \mathcal{F}_{\mathcal{RC}} \cdot \sin^4\left(\frac{q \cdot l}{2}\right) \tag{1}$$

Here ω describes the energy of the photons, m_ϕ describes the mass of the WISP, l is the length of the cavity, both in front of the wall and behind, C_{wisp} is the photon-WISP coupling, and $\mathcal{F}_{\mathcal{PC}}$ and $\mathcal{F}_{\mathcal{RC}}$ describe the finesse of the production and regeneration cavity, respectively. The variable q is defined as $q = |n\cdot\omega - \sqrt{\omega^2 - m_\phi^2}|$ where n is the index of refraction in the traversal path. If the coupling parameter of axion like particles is given by Eq. 2, then it can be seen how making the index of refraction 1, i.e. the traversal path is in vacuum, is a maximum for probability of conversion.

$$|C_{alp}|^2 = 4 \cdot \frac{(g_{a\gamma\gamma}\omega B)^2}{(m_\phi^2 + 2\omega^2(n-1))^2} \tag{2}$$

If Eq. 2 is substituted into Eq. 1 with the assumption that the path is in vacuum, n=1, and that $ql \ll 1$, then a simplified approximation of the probability in an LSW experiment is given in Eq. 3.

$$P_{\gamma\to\phi\to\gamma} = \frac{1}{16} \cdot \mathcal{F}_{\mathcal{PC}}\mathcal{F}_{\mathcal{RC}} \cdot (g_{a\gamma\gamma}Bl)^4 \tag{3}$$

From Eq. 3 it becomes very clear the variables that must be maximized in the ALPS experiment in order to maximize sensitivity. This derivation was taken from Graham *et al.*[3] section 5.1. By maximizing the finesse of the cavities, the experimental length, and the magnetic field strength, photon coupling strengths of lower magnitudes can be probed.

ALPS-IIc seeks to use a 200 m path length at DESY, and having this path be under a uniform 5.3 T magnetic field strength by using approximately 20 HERA dipole magnets. It is also planned to have an effective circulating power of 150 kW in the production cavity, and $\mathcal{F}_{\mathcal{RC}} = 40,000$ in the regeneration cavity, allowing probing of photon coupling strengths of $g_{a\gamma\gamma} = 2 \times 10^{-11} GeV^{-1}$ [Graham *et al.*[3]].

B. Effective Point of Reflection

In order to realize the needed sensitivity for ALPS-IIc, the production and regeneration cavities are required to be mode matched and phase locked to each other, and must maintain a condition of 95% power transmission throughout the experimental run time. The proposed ALPS-IIc setup requires using 532 nm light in the regeneration cavity, and using this green light to maintain this 95% power transmission for 1064 nm. Thus, the longitudinal modes of the cavities cannot drift by large amounts throughout the experimental run time, and this becomes an issue due to the reflection depth difference between 1064 nm and 532 nm light.

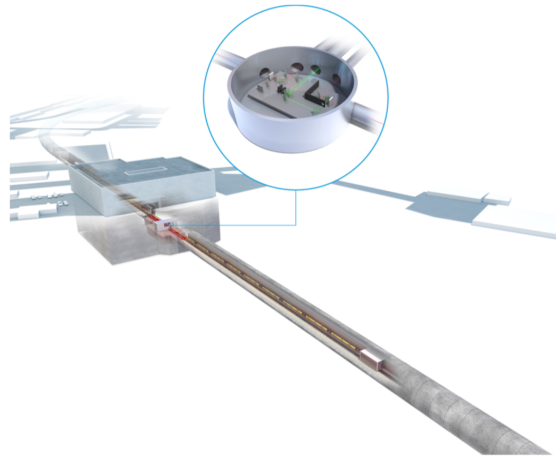

FIG. 3: Conceptual view of ALPS-II at DESY [Copyright 2013, DESY]

When reflecting different wavelengths of light from a medium, there are multiple effects that must be taken into account, such as phase-dispersion, reflection delay, and energy storage.[6] The reflection delay and energy storage is accounted for by defining a quantity called the "penetration depth" of a material, which is effectively the depth inside a mirror where the optical wave appears to reflect, or falls to $1/e$ of the impinging wave value.[6] This new penetration depth then affects the round trip path length of a EM wave, which is important to take into account in order to maintain the length and mode locking of the two cavities in ALPS-IIc.

If only a single cavity was being designed, accounting for this additional path length in construction of the cavity would be a trivial task. It would also be simple to experimentally design two cavities, each for a different wavelength (532 nm, 1064 nm), that are in resonance with each other. What presents an issue is that the penetration depths for each wavelength do not stay the same throughout experimental run times, thus creating a drift in the effective cavity lengths throughout the experiment. Since the 532 nm beam is being used to keep the 1064 nm beam in resonance for the regeneration cavity, the drifts between the two cannot become too large. If these drifts become too large, in the case of ALPS-IIc not being able to maintain a 95% power transmission overlap, then the design sensitivity will not be reached.

In order to meet this design requirement for ALPS-IIc, special mirror coatings were designed to meet this goal. Before these coatings can be employed, they must first be tested under similar conditions to that of the final setup, and at extremes that may occur during the final experiment, and this characterization is the goal of the Effective Point of Reflection experiment.

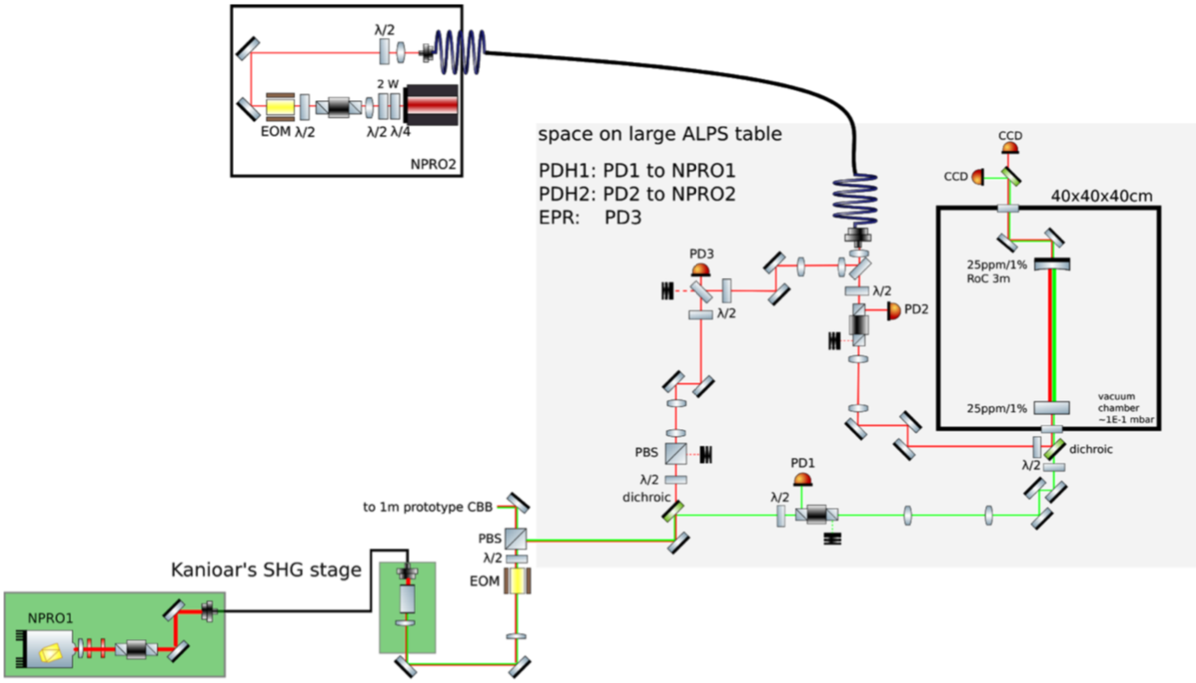

FIG. 4: Proposed Experimental Setup [Dennis Schmelzer]

II. PROPOSED SETUP

The proposed setup consists of two lasers feeding 1064 nm and 532 nm light into a static cavity, as shown in Fig. 4. Using PDH (Pound-Drever-Hall) frequency stabilization[7], both lasers can be frequency stabilized to the effective cavity length for that wavelength. Both lasers initially put out 1064 nm light, so each laser is stabilizing the 1064 nm output to the length of the cavity.

NPRO1(Non-planar-ring-oscillator) goes through a single pass PPKTP SHG(Second Harmonic Generation) stage where approximately 150 µW of the light is frequency doubled to 532 nm and then directed towards the cavity. NPRO2 does not undergo an SHG stage, so it inputs only 1064 nm light into the cavity, at a proposed power level of approximately 800 µW. The 1064 nm portion of the NPRO1 beam is brought out and directed to PD3 (Photodetector 3), along with a portion of the beam from NPRO2.

What this setup allows is that due to both wavelengths seeing a different effective length of the cavity, through the use of PDH frequency stabilization, each laser is frequency stabilized to slightly different frequencies. This allows the 1064 nm beams that were split away before entering the cavity to be superimposed on PD3, and due to the slight frequency difference, produce a beat frequency. This beat frequency then directly corresponds to the static EPR difference between 1064 nm and 532 nm light in the cavity, and when conditions are changed in the cavity, the change in beat frequency also corresponds to the ΔEPR.

The optics present in each of the beam paths are needed in order to properly polarize the beams and mode match them to the cavity. Both paths need to make use of an EOM for modulating the frequency for the PDH lock, and the Faraday Isolators serve the purpose of not only preventing back reflections from destabilizing the laser output, but also to redirect the reflected light onto either PD1 or PD2 where it can be detected for the PDH lock. Both beams are brought into the vacuum chamber through windows, where they impact a 27 cm rigid spacer cavity that has a flat mirror combined with a 2 m radius of curvature mirror, having an overall cavity finesse of approximately 60000 for 1064 nm and 300 for 532 nm. The beam in transmission of the cavity is then brought out of the chamber, and split so each wavelength is impinging on its own photodiode.

Using this method, many things about the EPR of the cavity can be investigated without greatly changing the setup. Time measurements of the ΔEPR can be made in order to see how the mirror coatings will act under run times similar to that of the final ALPS-IIc run time, the power inputted into the cavity can be varied in order to understand the effect of power on the ΔEPR of the substrates, the temperature of the cavity can be changed through application of a heating element to the outside of the cavity, the planar mirror can be laterally moved in order to test substrate homogeneity across the mirror, and the radius of curvature for the mirror can also be changed by exchanging it with a 3m RoC mirror.

Although all of the above can be used to categorize the mirrors, the most important measurement to be made is the temperature dependence of the ΔEPR. Using the simulated coating values from University of Florida and

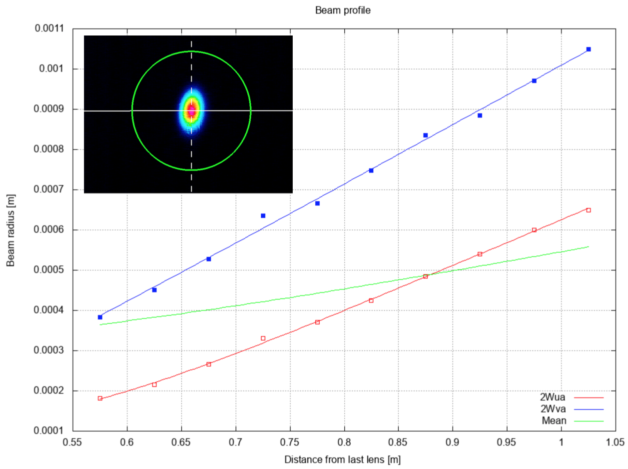

FIG. 5: Far-field measurement of 532 nm beam

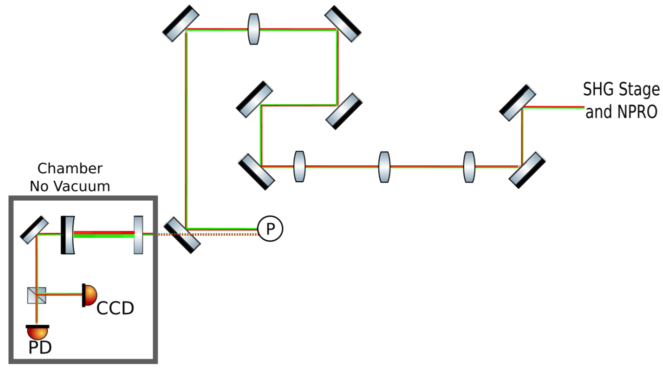

FIG. 6: Static EPR Setup

the design temperature stability of 0.2 K that can be maintained throughout the experimental run time, Eq. 4 can give the values of required ΔEPR length stability per mirror.

$$\frac{d\Delta EPR}{dT} \cdot \Delta T < 0.5\,\mathrm{pm} \tag{4}$$

III. PROGRESS REPORT

Upon arrival to AEI, the proposed setup above had been theorized, the rigid spacer cavity had been built along with the necessary mounts, and the vacuum chamber had been built and placed. The optical paths, mode matching, fiber coupling, beam detection, and PDH locks were not in place. Work began with creating the mode matching for the 532 nm beam path, preparing and placing all the mirrors and lens's, and measuring the beam width along the optical path. This was done through the use of a WinCamD from DataRay and gaussian fitting programs in order to investigate how well the actual beam was fitting to the theoretical mode matching.

A capture from a WinCamD and a gaussian fit of the beam can be shown in Fig. 5, showcasing an issue that caused a delay in the implementation of the green path. The beam had an intense ellipticity, and this made categorizing the waist size and position difficult, as the astigmatism created a size and position for both axes of the beam. This issue was traced back to the fiber collimated beam not hitting the PPKTP crystal correctly at the SHG stage, and was fixed and work continued.

After the mirror and lenses were placed for the 532 nm path, it was decided that obtaining a measurement of the static EPR of the cavity would be a useful first step, so the dichroic was removed from the 532 nm path, essentially producing a dual beam of 532 nm and 1064 nm mode-matching into the cavity (which naturally gives poor mode-matching for 1064 nm due to it being designed for 532 nm), and then the beam was aligned to the cavity. A CCD and PD were placed inside the vacuum chamber after the cavity in order to monitor the flashes through the cavity of the TEM_{00} mode for both 532 nm and 1064 nm. This setup is shown in Fig. 6. Actuating on the PZT (piezoelectric actuator) of the laser allowed frequency scanning of the cavity, which allows locating the TEM_{00} mode for the 532 nm beam and determining the FSR (free spectral range) of the cavity. Due to the intensity of the 532 nm beam being significantly higher than that of the 1064 nm beam, after the location of the TEM_{00} mode for 532 nm was found and the voltage on the PZT was recorded, a filter was placed in the path to filter out 532 nm and then the fundamental mode of 1064 nm could be found and its corresponding voltage recorded.

From this, it was determined that the static EPR difference between the green and infrared beam was 133nm (-7%, +22%). This corresponds to a frequency offset of approximately 140 MHz, which differs from the simulated values for these coatings of 207 MHz, but this does not necessarily matter as the accuracy of static EPR difference measurement does not matter, only the accuracy of the change in ΔEPR measurement. This measurement of approximately 140 MHz also means that the photodiodes and the connected frequency counter for detecting the beat overlap for the change in ΔEPR on PD3 must be high speed.

During this time an issue arose with one of the tables isolation feet breaking, causing the table to lose isolation. This was a multiple day delay as the new part not only needed to be ordered, but the entire table required being jacked up to allow the foot to be removed and the ripped part replaced. After the replacement, pressure was restored to the table and the optical table could be isolated again.

After obtaining this initial measurement, we continued on working towards the proposed setup. The EOM and Faraday Isolator for the green beam were placed, and the cavity was aligned for only green. Two primary issues arose during the alignment of the EOM, the main one being that the beam seemed to drift over small periods of time, causing the EOM to begin to clip causing beam distortion. After a short investigation, it was found that

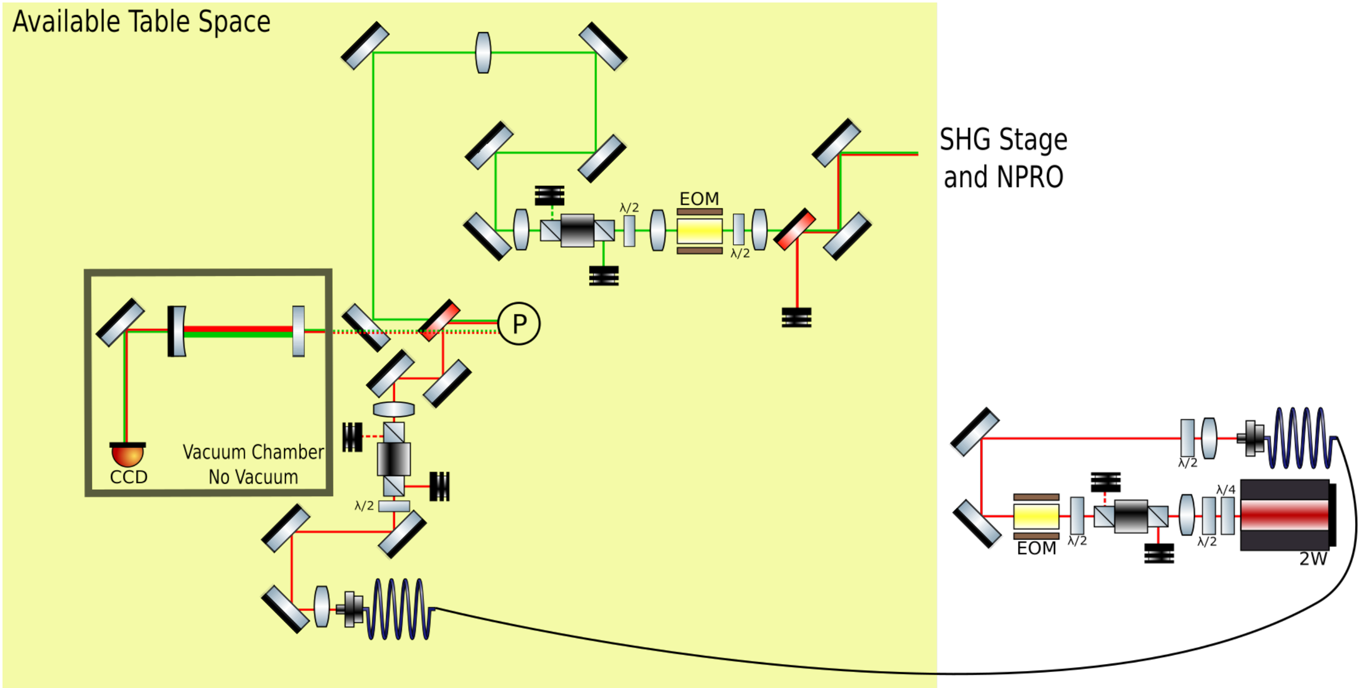

FIG. 7: Current EPR Setup [31.07.2018]

one of the mirrors in the stage before the pickup (in Fig. 6 the area titled "SHG Stage and NPRO") was not fully tightened, so the mirror had the ability to slightly rotate, thus causing the clipping.

Also, during alignment of the EOM with the WinCamD, it was found that there were random large changes in the intensity of the beam, thus making alignment very difficult. After a short investigation, it was found that the SHG PPKTP temperature cable was frayed and broken at the controller such that any movement to the cable would cause a temperature change in the crystal causing the intensity fluctuations. The cable was replaced, and the EOM was able to be aligned.

The 1064 nm beam was fiber coupled with approximately 70% efficiency. This efficiency is more than sufficient for this experiment, providing approximately 4 mW currently compared to the design power of 600 µW.

After fiber coupling the 1064 nm beam, the mode matching was put into place along with all of the necessary mirrors, and the beam was brought into the cavity and aligned. The 532 nm beam was blocked during this process to allow easy identification of the 1064 nm beam on the CCD, and after alignment was complete the 532 nm beam was unblocked and both beams were flashing through the cavity. This was the last thing able to be done at AEI before departure, and the final setup upon exit is shown in Fig. 7.

IV. FUTURE WORK

The work that still needs to be done is mainly centered on installing the control electronics for the Pound-Drever-Hall frequency control, and installing the EPR beat path. The photodiodes for the reflected portions of both the 532 nm and 1064 nm paths must be installed, and the all of the control electronics that bring this information back the respective lasers must be done. The EPR beat path must be installed and optimized in order to allow overlap on PD3. PD3 and the resulting frequency counter electronics must be high speed in order to handle the 140-200MHz predicted from the static EPR measurement and simulations.

V. ACKNOWLEDGMENTS

I would like to extend my deepest thanks to Dennis for not only for his immense help on the project, but also for his assistance in adapting to Germany. I would also like to thank Benno, Kanioar, and Li-Wei for welcoming me into their lab and their kind assistance. Finally, I would like to thank Guido Mueller, Bernard Whiting, Kristin Nichola, Michaela Pickenpack, and Andrew Miller for giving me this opportunity and helping to make this program what it is, and the NSF for funding this opportunity.

[1] R. D. Peccei and H. R. Quinn, "CP conservation in the presence of pseudoparticles," Phys. Rev. Lett. **38**, 1440–1443 (1977).

[2] J. E. Kim and G. Carosi, "Axions and the strong *cp* problem," Rev. Mod. Phys. **82**, 557–601 (2010).

[3]P. W. Graham, I. G. Irastorza, S. K. Lamoreaux, A. Lindner, and K. A. van Bibber, "Experimental searches for the axion and axion-like particles," Annual Review of Nuclear and Particle Science **65**, 485–514 (2015).

[4]P. Sikivie, D. B. Tanner, and K. van Bibber, "Resonantly enhanced axion-photon regeneration," Phys. Rev. Lett. **98**, 172002 (2007).

[5]K. Ehret, M. Frede, S. Ghazaryan, M. Hildebrandt, E.-A. Knabbe, D. Kracht, A. Lindner, J. List, T. Meier, N. Meyer, D. Notz, J. Redondo, A. Ringwald, G. Wiedemann, and B. Willke, "Resonant laser power build-up in alpsa light shining through a wall experiment," Nuclear Instruments and Methods in Physics Research Section A: Accelerators, Spectrometers, Detectors and Associated Equipment **612**, 83 – 96 (2009).

[6]D. Babic and S. Corzine, "Analytic expressions for the reflection delay, penetration depth, and absorptance of quarter-wave dielectric mirrors," IEEE Journal of Quantum Optics **28**, 514–524 (1992).

[7]E. D. Black, "An introduction to pound-drever-hall laser frequency stabilization," American Journal of Physics **69**, 79–87 (2001), https://doi.org/10.1119/1.1286663.